Sciencexpress Research Articles

# The protein LEM promotes CD8$^+$ T cell immunity through effects on mitochondrial respiration

**Isobel Okoye,[1]* Lihui Wang,[1]* Katharina Pallmer,[2] Kirsten Richter,[2] Takahuru Ichimura,[3] Robert Haas,[4] Josh Crouse,[2] Onjee Choi,[1] Dean Heathcote,[1] Elena Lovo,[1] Claudio Mauro,[4] Reza Abdi,[3] Annette Oxenius,[2] Sophie Rutschmann,[1†] Philip G. Ashton-Rickardt[1,3‡]**

[1]Section of Immunobiology, Division of Inflammation and Immunology, Department of Medicine, Faculty of Medicine, Imperial College London, Exhibition Road, London SW72AZ, UK. [2]Institute of Microbiology, ETH Zurich, Vladimir-Prelog-Weg 1-5/10, 8093, Zurich, Switzerland. [3]Transplantation Research Center, Brigham and Women's Hospital, Harvard Medical School, 221 Longwood Avenue, Boston MA 02215, USA. [4]William Harvey Research Institute, Barts and The London School of Medicine and Dentistry, Queen Mary University of London, London EC1M 6BQ, UK.

*These authors contributed equally to this work.

†Present address: Section of Molecular Immunology, Division of Inflammation and Immunology, Department of Medicine, Faculty of Medicine, Imperial College London, Du Cane Road, London W12 0NN, UK.

‡Corresponding author. E-mail: p.ashton-rickardt@imperial.ac.uk

**Protective CD8$^+$ T cell–mediated immunity requires a massive expansion in cell number and the development of long-lived memory cells. Using forward genetics in mice, we identified an orphan protein named Lymphocyte Expansion Molecule (LEM) that promoted antigen-dependent CD8$^+$ T cell proliferation, effector function, and memory cell generation in response to infection with lymphocytic choriomeningitis virus. Generation of LEM-deficient mice confirmed these results. Through interaction with CR6 interacting factor (CRIF1), LEM controlled the levels of oxidative phosphorylation (OXPHOS) complexes and respiration resulting in the production of pro-proliferative mitochondrial Reactive Oxygen Species (mROS). LEM provides a link between immune activation and the expansion of protective CD8$^+$ T cells driven by OXPHOS and represents a pathway for the restoration of long-term protective immunity based on metabolically modified CTL.**

Cytotoxic CD8$^+$ T cells (CTL) are a central arm of the immune system responsible for protection from intracellular viruses and cancer because they kill infected or transformed cells (*1*). Since chronic virus infection (*2*) and cancer (*3*) are widespread diseases, it is clear that CTL-immunity often fails. A major reason for this failure is because high viral (*4*, *5*) or tumor (*6–8*) load results in either deletion or functional inactivation (known as immune exhaustion) of CTL. The result is failure in both short-term CTL immunity and immunological memory because memory CD8 T cell development is blocked (*9*). Impaired expansion is an important cause of deletion and immune exhaustion and results in the failure to produce sufficient numbers of protective CTL and memory cells (*5*).

### *Retro* mutant mice have increased immunity to chronic viral infection

Infection of wild-type C57BL/6 mice with the clone 13 variant of lymphocytic choriomeningitis virus (LCMV C13) is an established model for human chronic viral infection resulting in a massive viral load that causes both deletion and immune exhaustion of CTL and a block in memory CD8 T cell development (*10*).

We examined the CTL response to LCMV C13 infection after germ-line mutagenesis to identify mutants with enhanced immunity. To this end, 430 third-generation (G3) ethyl-N-nitrosourea (ENU)-induced germ-line mutants were produced in a C57BL/6J background (*11*). G3 mice were infected with LCMV C13 and after 8 days the level of LCMV-specific CD8 T cells measured in the spleen by staining with a tetramer for the np396 LCMV peptide and flow-cytometry (*12*). Three independent germ-line transmissible modifications, which resulted in increased levels of LCMV-specific CD8 T cells were isolated, of which one (a semi-dominant) was bred to homozygosity (fig. S1A). We named this strain *Retro*.

Homozygous *Retro* mutant mice showed a 10-fold increase in CD8 T cells specific for LCMV np396 peptide compared to wild-type (WT) and a smaller but significant increase in the number of CTL specific for the gp33-LCMV peptide (Fig. 1, A and B). Compared to WT mice, a smaller percentage of *Retro* mutant CTL expressed the Programmed Cell Death-1 (PD-1) immune exhaustion marker (*5*) (Fig. 1C). However, *Retro* mutant mice still harbored increased numbers of PD-1$^+$ np396$^+$ CD8$^+$ cells compared to WT (Fig. 1D). In addition, *Retro* mutant CTL exhibited increased functionality: there was increased CTL activity in ex vivo killing experiments (Fig. 1E), increased exocytosis of cytotoxic granules (*11*) (Fig. 1F), and increased production of the cyto-

kine interferon (IFN)-γ (fig. S1B). The increase in CTL immunity resulted in a $10^6$-fold decrease in LCMV C13 titer in the spleens of *Retro* mutant mice on day 8 after infection compared to WT (Fig. 1G). The increase in CTL activity was a function of cell number (fig. S1C).

All *Retro* mutant mice succumbed to LCMV C13 infection after 14 days whereas all WT mice had survived (Fig. 1H). *Retro* mutant death is presumably a consequence of elevated CTL-mediated cytolysis resulting in the fatal loss of vascular integrity (*13*). Despite an increase in activated phenotype T cells (fig. S2), viability, blood development and autoimmunity in *Retro* mutant mice was normal (fig. S3 and tables S1 to S3). In vivo BrdU labeling indicated that np396$^+$ CD8$^+$ cells underwent increased proliferation after LCMV C13 infection of *Retro* mutant mice (Fig. 1I). The increased number of antigen-specific CD8 T cells in LCMV C13-infected *Retro* mutant mice is likely due to increased proliferation of these cells.

Adoptive transfer of *Retro* mutant CD8 T cells (*14*), showed that the phenotype of increased CTL-immunity resides in the CD8 T cell compartment (fig. S4, A to D). The phenotype of *Retro* mutant mice also extended to anti-tumor responses. After challenge with B16 F10 melanoma cells, *Retro* mutant mice harbored 3-fold more CTL (Fig. 2A) and 4-fold fewer tumors (Fig. 2, B and C).

### *Retro* mutant mice have increased memory T cell development

After acute infection of *Retro* mutant mice with LCMV Armstrong there was an increase in the clonal burst size of both np396$^+$ CD8$^+$ and gp33$^+$ CD8$^+$ cells (Fig. 2, D and E) compared to WT. Longitudinal analysis in the blood revealed a corresponding increase in the number of LCMV-specific CD8 T cells during the memory phase in *Retro* mutant mice (*15*). After 70 days, there was a 4-fold increase in the number of LCMV-specific central memory T CD8 cells (Tcm) in the spleen as identified by the CD62L$^+$ CD127$^+$ CD8$^+$ cell surface phenotype (*16*) (fig. S4, E and F).

We boosted mice with a second dose of LCMV Armstrong and measured the expansion of secondary CTL during the memory response. The numbers of secondary CTL were about 10-fold higher compared to WT (fig. S4, G and H) indicating that *Retro* mutant mice have an enhanced memory phenotype. During acute immune responses the pool of CTL contains not only short-lived effectors but also memory cell precursors (*17*, *18*). The increase in the total number of CD8 T cells resulted in an increase in the number and percentage of both memory cell precursors and short-lived effectors in *Retro* mutants compared to WT (fig. S5). Therefore the *Retro* mutation increases the level of both primary short-lived effectors and Tcm by facilitating a global increase in the expansion of antigen-activated CD8 T cells.

### The *Retro* mutation identifies Lymphocyte Expansion Molecule

We used high-throughput exome sequencing (*19*) to identify the *Retro* mutation. Comparison with the reference C57BL/6J genome identified several homozygous single nucleotide variants (SNV) in homozygous *Retro* mutant mice (fig. S6A). Upon re-sequencing and comparison with the Charles River sub-strain of C57BL/6J used for our ENU mutagenesis, four homozygous SNVs were identified as being associated with *Retro* homozygous mutant mice. Only one homozygous SNV correlated with the *Retro* homozygous phenotype (fig. S6B). This was an A to G transition of nucleotide 1304 (A1304G) in exon 2 of the *BC055111* gene on chromosome 4 (fig. S7A). *BC055111* encodes an orphan protein with no significant homology to any other mouse protein (BLASTP: *E* value > 0.38). The *BC055111*$^{Retro}$ allele (R) was semi-dominant for increased CTL immunity to LCMV C13 (fig. S7, B to D).

We generated C57BL/6 mice with a *BC055111* knock-out (KO) allele (*20*) (fig. S8). Homozygosity for the *BC055111* KO allele results in embryonic lethality and so we used heterozygous KO mice to validate the gene candidate (*12*). There was decreased *BC055111*-encoded protein in CTL from heterozygous *BC055111 KO* mice compared to WT (Fig. 3, A and B). We observed decreased np396$^+$ CD8$^+$ expansion (Fig. 3C), increased LCMV titer (Fig. 3D) and decreased CTL activity (Fig. 3E) in *BC055111* $^{W/KO}$ compared to *BC055111*$^{W/W}$ mice. Therefore *BC055111* directly controls CTL immunity to LCMV . We named the *BC055111* encoded orphan protein Lymphocyte Expansion Molecule (LEM).

### The *Retro* mutation stabilizes *Lem* mRNA

The kinetics of *Lem* mRNA accumulation in *Retro* mutant CD8 T cells after LCMV C13 infection was increased compared to WT (Fig. 3F). The increased level of *Lem* mRNA was also observed when transcription was inhibited by actinomycin D, indicating that the *Retro* mutation stabilized *Lem* mRNA in CD8 T cells (Fig. 3G).

*Lem* mRNA contains introns in the 3′ un-translated region (3′-UTR), which may make it susceptible to Nonsense mediated decay (NMD) (*21*). This was confirmed when blockade of NMD by emetine increased the stability of wild-type *Lem* mRNA (Fig. 3G). The *Retro* mutation is predicted to abolish an Alternative splice factor/Splice factor 2 (ASF/SF2) binding site in *Lem* (*12*), which is thought to be required for NMD (*22*). Immunoprecipitation (IP) confirmed decreased levels of SF2 associated with *Retro* mutant *Lem* message (Fig. 3H) in cells with normal SF2 levels (Fig. 3I). This suggests that the A1304G mutation in *Retro* mutant mice partially protects *Lem* mRNA from NMD resulting in stabilization. The *Lem* open-reading frame (ORF) harboring the *Retro* A1304G mutation was no better than WT ORF at

driving interleukin (IL)-2 induced proliferation of T cells (fig. S9 and Fig. 3J). Therefore, the increased expression of *Lem* rather than any qualitative alteration in protein activity is responsible for the phenotype of *Retro* mutant mice. We conclude that WT LEM is a positive modulator of CTL expansion that is up-regulated in *Retro* mutant mice.

**The *Retro* mutation increases LEM expression**

LEM protein was up-regulated in total CD8 T cells after LCMV C13 infection with *Retro* mutant mice displaying increased kinetics compared to WT (Fig. 4, A and B). Intracellular staining (ICS) (fig. S10) indicated that LEM expression was specific for activated CD8 T cells ($CD44^{hi}$ $CD62L^{lo}$ $CD8^{+}$) and was elevated in *Retro* mutant cells (Fig. 4, C and D). LEM was up-regulated 2 days after LCMV C13 infection despite a low frequency of CD8 cells expressing LCMV-specific TCRs (fig. S11A and Fig. 4, A and C). In addition to stimulation through the TCR (via anti-CD3 antibody) (Fig. 4E), treatment with either IL-2 (Fig. 4F) or IL-15 (Fig. 4G) resulted in LEM up-regulation, which was enhanced in *Retro* mutant CD8 T cells (Fig. 4, E to G). Therefore, LEM expression can be induced by bystander activation by pro-proliferative cytokines as well as antigen-dependent TCR signals. The level of LEM controlled the levels of *Retro* mutant CD8 T cells both in *vivo* (fig. S11, B to E) and in vitro (fig. S12). PD-1 up-regulation by *Retro* mutant CTL was un-affected in vitro after TCR-stimulation suggesting that LEM does not directly down-regulate PD-1 expression (fig. S11, F and G).

**Functional equivalence of human LEM**

*C1ORF177* encodes the human homolog of LEM (BLASTP: 72% of complete amino acid identity with mouse LEM, *E* value = 0), which is up-regulated in activated human CD8 T cells (Fig. 4, H and I). Ectopic expression of human-LEM resulted in about a 15-fold increase in the expansion (Fig. 4J). Therefore, LEM can modulate CD8 T cell expansion in man as well as mice.

**LEM interacts with CRIF1 to control the activity of OXPHOS proteins**

Analysis of LEM amino acid sequence predicts the presence of at least two intrinsically unstructured (IU) protein domains (*12*, *23*). Therefore we investigated whether LEM modulates CD8 T cell proliferation through specific protein: protein interactions. Yeast two-hybrid (Y2H) analysis identified 9 different LEM-interacting proteins (*24*)) (fig. S13). Co-immunoprecipitation (co-IP) with anti-LEM antibody (fig. S10), demonstrated that one target – CR6 interacting factor (CRIF1) interacts with LEM in CTL (Fig. 5, A and B).

CRIF1 is required for the translation and insertion of oxidative phosphorylation (OXPHOS) polypeptides into the inner membrane of mitochondria after they emerge from the 39S subunit of the mitoribosomes (*25*). Confocal immunofluorescence microscopy (CIM) revealed that LEM co-localizes with CRIF1 in CTL (Fig. 5, C and D, and fig. S14). Both LEM and CRIF1 were localized to mitochondria by co-staining with the mitotracker red dye (figs. S15 and S16). Co-IP localized LEM to the mitoribosome by revealing an association with the 39S subunit protein MRPL23 and several OXPHOS proteins such as NADH ubiquinone oxidoreductase chain 1 (ND1), ubiquninol cytochrome c oxidoreductase chain 2 (UQCRC2) and cytochrome c oxidoreductase chain 1 (COX1) (*25*) (Fig. 5E). The OXPHOS protein ATP synthase $\alpha$ subunit 1 (ATP5A1) does not require CRIF1 for translation and did not co-IP, suggesting that interaction of LEM with OXPHOS proteins is via CRIF1. Through its interaction with CRIF, LEM is part of a complex that mediates the translation and insertion of OXPHOS proteins into the mitochondrial inner membrane.

*Retro* mutant CTL harbored increased levels and heterozygous LEM KO CTL reduced levels of OXPHOS proteins (Fig. 5, F and G). Immuno-capture confirmed that the specific activities of OXPHOS complexes were elevated in *Retro* mutant CTL (Fig. 5, H and I); although LEM did not affect the expression of *Oxphos* genes or the number or mass of mitochondria (fig. S17, A to C). Therefore, LEM controlled the activity of OXPHOS complexes by most likely facilitating the production of sub-unit proteins.

As was observed in CRIF1 KO cells (*25*), when we knocked down *Crif1* mRNA (fig. S18, A to C), OXPHOS specific activity was reduced (Fig. 5, J and K). Knock-down of *Crif1* message in *Retro* mutant CTL also abolished the increases in OXPHOS activity due to LEM up-regulation. We conclude that LEM interaction with CRIF1 within mitochondria determines OXPHOS activity.

CRIF1 is required for cell proliferation during embryo development (*26*). *Crif1* message knock-down resulted in the impaired proliferation and expansion of anti-LCMV CTL (fig. S18, D and E). The increase in CTL expansion caused by LEM up-regulation required CRIF1 expression because *Crif1* message knock-down diminished the increased expansion of *Retro* mutant CTL. We conclude that LEM requires interaction with CRIF1 to drive the expansion of CTL.

**LEM is a positive modulator of mitochondrial ROS-driven proliferation**

We examined the consequences of LEM control of OXPHOS activity on CTL metabolism and expansion. Oxygen consumption studies demonstrated that *Retro* mutant CTL had significantly higher respiratory levels compared to WT (Fig. 6A) (*27*) but glycolysis was not increased (fig. S17D). Conversely, respiratory activity (Fig. 6B) of LEM heterozygous KO CTL but not glycolysis (fig. S17E) was decreased.

OXPHOS results in the production reactive oxygen species (ROS) through stepwise reduction of $O_2$ (*27*). The modulation of OXPHOS by LEM resulted in altered production of mROS. Staining with the redox sensitive dye MitoSOX red revealed that compared to WT, *Retro* mutant CTL had increased levels of mitochondrial ROS (mROS) and LEM heterozygous KO CTL had decreased mROS (Fig. 6C). The

production of mROS is required for the activation and expansion of T lymphocytes (*27*). Injection of *Retro* mutant mice with the antioxidant MnTBAP (*28*) reduced the level of mROS in CTL (Fig. 6D) resulting in decreased proliferation (Fig. 6E) and expansion of CTL (Fig. 6F) with a corresponding increase in LCMV C13 titer (Fig. 6G). We conclude that mROS resulting from OXPHOS activity drives expansion and CTL immunity in *Retro* mutant mice.

We have used unbiased forward genetics to discover LEM at the heart of a pathway that, when up-regulated not only restores CTL immunity to chronic viral infection and tumor challenge but also increases memory cell development. Although other molecular interventions either restore primary CTL immunity (*5*) or divert development toward the memory lineage (*29*) the LEM pathway is important because it controls the expansion of both short-term effectors and memory cells (*9*). Up-regulation of LEM in *Retro* mutant mice increased both the overall number of CTL and also the number of PD-1$^{+}$ CTL. Therefore LEM therapy has the potential to both globally expand CTL and to increase the number of PD-1$^{+}$ CTL available for de-repression by anti-PD-1 antibodies (*8*).

At the peptide tunnel exit of 39S mitoribosomes, LEM is likely recruited by CRIF1 to facilitate the insertion of OXPHOS polypeptides into the inner mitochondrial membrane, thereby controlling OXPHOS activity (*25*) (fig. S19). We propose that CTL expansion and memory cell development are controlled by mROS produced after the up-regulation of LEM upon immune activation (*27*, *30*)

## REFERENCES AND NOTES


1. J. H. Russell, T. J. Ley, Lymphocyte-mediated cytotoxicity. *Annu. Rev. Immunol.* **20**, 323–370 (2002). Medline doi:10.1146/annurev.immunol.20.100201.131730
2. B. Autran, G. Carcelain, B. Combadiere, P. Debre, Therapeutic vaccines for chronic infections. *Science* **305**, 205–208 (2004). Medline doi:10.1126/science.1100600
3. D. Pardoll, T cells take aim at cancer. *Proc. Natl. Acad. Sci. U.S.A.* **99**, 15840–15842 (2002). Medline doi:10.1073/pnas.262669499
4. C. L. Day, D. E. Kaufmann, P. Kiepiela, J. A. Brown, E. S. Moodley, S. Reddy, E. W. Mackey, J. D. Miller, A. J. Leslie, C. DePierres, Z. Mncube, J. Duraiswamy, B. Zhu, Q. Eichbaum, M. Altfeld, E. J. Wherry, H. M. Coovadia, P. J. Goulder, P. Klenerman, R. Ahmed, G. J. Freeman, B. D. Walker, PD-1 expression on HIV-specific T cells is associated with T-cell exhaustion and disease progression. *Nature* **443**, 350–354 (2006). Medline doi:10.1038/nature05115
5. D. L. Barber, E. J. Wherry, D. Masopust, B. Zhu, J. P. Allison, A. H. Sharpe, G. J. Freeman, R. Ahmed, Restoring function in exhausted CD8 T cells during chronic viral infection. *Nature* **439**, 682–687 (2006). Medline doi:10.1038/nature04444
6. M. A. Curran, W. Montalvo, H. Yagita, J. P. Allison, PD-1 and CTLA-4 combination blockade expands infiltrating T cells and reduces regulatory T and myeloid cells within B16 melanoma tumors. *Proc. Natl. Acad. Sci. U.S.A.* **107**, 4275–4280 (2010). Medline doi:10.1073/pnas.0915174107
7. P. Georgel, X. Du, K. Hoebe, B. Beutler, ENU mutagenesis in mice. *Methods Mol. Biol.* **415**, 1–16 (2008). Medline
8. S. L. Topalian, F. S. Hodi, J. R. Brahmer, S. N. Gettinger, D. C. Smith, D. F. McDermott, J. D. Powderly, R. D. Carvajal, J. A. Sosman, M. B. Atkins, P. D. Leming, D. R. Spigel, S. J. Antonia, L. Horn, C. G. Drake, D. M. Pardoll, L. Chen, W. H. Sharfman, R. A. Anders, J. M. Taube, T. L. McMiller, H. Xu, A. J. Korman, M. Jure-Kunkel, S. Agrawal, D. McDonald, G. D. Kollia, A. Gupta, J. M. Wigginton, M. Sznol, Safety, activity, and immune correlates of anti-PD-1 antibody in cancer. *N. Engl. J. Med.* **366**, 2443–2454 (2012). Medline doi:10.1056/NEJMoa1200690
9. M. A. Williams, M. J. Bevan, Effector and memory CTL differentiation. *Annu. Rev. Immunol.* **25**, 171–192 (2007). Medline doi:10.1146/annurev.immunol.25.022106.141548
10. S. N. Mueller, R. Ahmed, High antigen levels are the cause of T cell exhaustion during chronic viral infection. *Proc. Natl. Acad. Sci. U.S.A.* **106**, 8623–8628 (2009). Medline doi:10.1073/pnas.0809818106
11. O. Choi, D. A. Heathcote, K. K. Ho, P. J. Müller, H. Ghani, E. W. Lam, P. G. Ashton-Rickardt, S. Rutschmann, A deficiency in nucleoside salvage impairs murine lymphocyte development, homeostasis, and survival. *J. Immunol.* **188**, 3920–3927 (2012). Medline doi:10.4049/jimmunol.1102587
12. Materials and methods are available as supplementary materials on *Science* Online.
13. H. Frebel, V. Nindl, R. A. Schuepbach, T. Braunschweiler, K. Richter, J. Vogel, C. A. Wagner, D. Loffing-Cueni, M. Kurrer, B. Ludewig, A. Oxenius, Programmed death 1 protects from fatal circulatory failure during systemic virus infection of mice. *J. Exp. Med.* **209**, 2485–2499 (2012). Medline doi:10.1084/jem.20121015
14. A. H. Rahman, W. Cui, D. F. Larosa, D. K. Taylor, J. Zhang, D. R. Goldstein, E. J. Wherry, S. M. Kaech, L. A. Turka, MyD88 plays a critical T cell-intrinsic role in supporting CD8 T cell expansion during acute lymphocytic choriomeningitis virus infection. *J. Immunol.* **181**, 3804–3810 (2008). Medline doi:10.4049/jimmunol.181.6.3804
15. L. L. Lau, B. D. Jamieson, T. Somasundaram, R. Ahmed, Cytotoxic T-cell memory without antigen. *Nature* **369**, 648–652 (1994). Medline doi:10.1038/369648a0
16. S. M. Byrne, A. Aucher, S. Alyahya, M. Elder, S. T. Olson, D. M. Davis, P. G. Ashton-Rickardt, Cathepsin B controls the persistence of memory CD8+ T lymphocytes. *J. Immunol.* **189**, 1133–1143 (2012). Medline doi:10.4049/jimmunol.1003406
17. J. T. Opferman, B. T. Ober, P. G. Ashton-Rickardt, Linear differentiation of cytotoxic effectors into memory T lymphocytes. *Science* **283**, 1745–1748 (1999). Medline doi:10.1126/science.283.5408.1745
18. N. S. Joshi, W. Cui, A. Chandele, H. K. Lee, D. R. Urso, J. Hagman, L. Gapin, S. M. Kaech, Inflammation directs memory precursor and short-lived effector CD8(+) T cell fates via the graded expression of T-bet transcription factor. *Immunity* **27**, 281–295 (2007). Medline doi:10.1016/j.immuni.2007.07.010
19. H. Fairfield, G. J. Gilbert, M. Barter, R. R. Corrigan, M. Curtain, Y. Ding, M. D'Ascenzo, D. J. Gerhardt, C. He, W. Huang, T. Richmond, L. Rowe, F. J. Probst, D. E. Bergstrom, S. A. Murray, C. Bult, J. Richardson, B. T. Kile, I. Gut, J. Hager, S. Sigurdsson, E. Mauceli, F. Di Palma, K. Lindblad-Toh, M. L. Cunningham, T. C. Cox, M. J. Justice, M. S. Spector, S. W. Lowe, T. Albert, L. R. Donahue, J. Jeddeloh, J. Shendure, L. G. Reinholdt, Mutation discovery in mice by whole exome sequencing. *Genome Biol.* **12**, R86 (2011). Medline doi:10.1186/gb-2011-12-9-r86
20. W. C. Skarnes, B. Rosen, A. P. West, M. Koutsourakis, W. Bushell, V. Iyer, A. O. Mujica, M. Thomas, J. Harrow, T. Cox, D. Jackson, J. Severin, P. Biggs, J. Fu, M. Nefedov, P. J. de Jong, A. F. Stewart, A. Bradley, A conditional knockout resource for the genome-wide study of mouse gene function. *Nature* **474**, 337–342 (2011). Medline doi:10.1038/nature10163
21. I. Ivanov, K. C. Lo, L. Hawthorn, J. K. Cowell, Y. Ionov, Identifying candidate colon cancer tumor suppressor genes using inhibition of nonsense-mediated mRNA decay in colon cancer cells. *Oncogene* **26**, 2873–2884 (2007). Medline doi:10.1038/sj.onc.1210098
22. H. Sato, N. Hosoda, L. E. Maquat, Efficiency of the pioneer round of translation affects the cellular site of nonsense-mediated mRNA decay. *Mol. Cell* **29**, 255–262 (2008). Medline doi:10.1016/j.molcel.2007.12.009
23. H. J. Dyson, P. E. Wright, Intrinsically unstructured proteins and their functions. *Nat. Rev. Mol. Cell Biol.* **6**, 197–208 (2005). Medline doi:10.1038/nrm1589
24. C. W. Xu, A. R. Mendelsohn, R. Brent, Cells that register logical relationships among proteins. *Proc. Natl. Acad. Sci. U.S.A.* **94**, 12473–12478 (1997). Medline doi:10.1073/pnas.94.23.12473
25. S. J. Kim, M. C. Kwon, M. J. Ryu, H. K. Chung, S. Tadi, Y. K. Kim, J. M. Kim, S. H. Lee, J. H. Park, G. R. Kweon, S. W. Ryu, Y. S. Jo, C. H. Lee, H. Hatakeyama, Y. Goto, Y. H. Yim, J. Chung, Y. Y. Kong, M. Shong, CRIF1 is essential for the synthesis and insertion of oxidative phosphorylation polypeptides in the mammalian mitochondrial membrane. *Cell Metab.* **16**, 274–283 (2012). Medline doi:10.1016/j.cmet.2012.06.012
26. M. C. Kwon, B. K. Koo, J. S. Moon, Y. Y. Kim, K. C. Park, N. S. Kim, M. Y. Kwon, M. P. Kong, K. J. Yoon, S. K. Im, J. Ghim, Y. M. Han, S. K. Jang, M. Shong, Y. Y. Kong, Crif1 is a novel transcriptional coactivator of STAT3. *EMBO J.* **27**, 642–653 (2008). Medline doi:10.1038/sj.emboj.7601986

27. L. A. Sena, S. Li, A. Jairaman, M. Prakriya, T. Ezponda, D. A. Hildeman, C. R. Wang, P. T. Schumacker, J. D. Licht, H. Perlman, P. J. Bryce, N. S. Chandel, Mitochondria are required for antigen-specific T cell activation through reactive oxygen species signaling. *Immunity* **38**, 225–236 (2013). Medline doi:10.1016/j.immuni.2012.10.020
28. N. G. Laniewski, J. M. Grayson, Antioxidant treatment reduces expansion and contraction of antigen-specific CD8+ T cells during primary but not secondary viral infection. *J. Virol.* **78**, 11246–11257 (2004). Medline doi:10.1128/JVI.78.20.11246-11257.2004
29. K. Araki, A. P. Turner, V. O. Shaffer, S. Gangappa, S. A. Keller, M. F. Bachmann, C. P. Larsen, R. Ahmed, mTOR regulates memory CD8 T-cell differentiation. *Nature* **460**, 108–112 (2009). Medline doi:10.1038/nature08155
30. G. J. van der Windt, B. Everts, C. H. Chang, J. D. Curtis, T. C. Freitas, E. Amiel, E. J. Pearce, E. L. Pearce, Mitochondrial respiratory capacity is a critical regulator of CD8+ T cell memory development. *Immunity* **36**, 68–78 (2012). Medline doi:10.1016/j.immuni.2011.12.007
31. S. J. Pettitt, Q. Liang, X. Y. Rairdan, J. L. Moran, H. M. Prosser, D. R. Beier, K. C. Lloyd, A. Bradley, W. C. Skarnes, Agouti C57BL/6N embryonic stem cells for mouse genetic resources. *Nat. Methods* **6**, 493–495 (2009). Medline doi:10.1038/nmeth.1342
32. M. M. McCausland, S. Crotty, Quantitative PCR technique for detecting lymphocytic choriomeningitis virus in vivo. *J. Virol. Methods* **147**, 167–176 (2008). Medline doi:10.1016/j.jviromet.2007.08.025
33. M. Zhang, S. M. Park, Y. Wang, R. Shah, N. Liu, A. E. Murmann, C. R. Wang, M. E. Peter, P. G. Ashton-Rickardt, Serine protease inhibitor 6 protects cytotoxic T cells from self-inflicted injury by ensuring the integrity of cytotoxic granules. *Immunity* **24**, 451–461 (2006). Medline doi:10.1016/j.immuni.2006.02.002
34. Y. Agata, A. Kawasaki, H. Nishimura, Y. Ishida, T. Tsubata, H. Yagita, T. Honjo, Expression of the PD-1 antigen on the surface of stimulated mouse T and B lymphocytes. *Int. Immunol.* **8**, 765–772 (1996). Medline doi:10.1093/intimm/8.5.765
35. N. Liu, T. Phillips, M. Zhang, Y. Wang, J. T. Opferman, R. Shah, P. G. Ashton-Rickardt, Serine protease inhibitor 2A is a protective factor for memory T cell development. *Nat. Immunol.* **5**, 919–926 (2004). Medline doi:10.1038/ni1107
36. A. J. Gehring, S. A. Xue, Z. Z. Ho, D. Teoh, C. Ruedl, A. Chia, S. Koh, S. G. Lim, M. K. Maini, H. Stauss, A. Bertoletti, Engineering virus-specific T cells that target HBV infected hepatocytes and hepatocellular carcinoma cell lines. *J. Hepatol.* **55**, 103–110 (2011). Medline doi:10.1016/j.jhep.2010.10.025
37. M. D. Brand, D. G. Nicholls, Assessing mitochondrial dysfunction in cells. *Biochem. J.* **435**, 297–312 (2011). Medline doi:10.1042/BJ20110162
38. C. Petrovas, Y. M. Mueller, I. D. Dimitriou, S. R. Altork, A. Banerjee, P. Sklar, K. C. Mounzer, J. D. Altman, P. D. Katsikis, Increased mitochondrial mass characterizes the survival defect of HIV-specific CD8(+) T cells. *Blood* **109**, 2505–2513 (2007). Medline doi:10.1182/blood-2006-05-021626

## ACKNOWLEDGMENTS

We thank C. Bangham and R. Shattock for helpful comments on the paper. The data reported in this manuscript are tabulated in the main paper and in the supplementary materials. The *Lem* gene sequence is deposited in Genebank Accession KP939367. P.G.A-R is the inventor on international patent application PCT/GB2014/051603 (International Publication Number WO 2014/188220) A1. The patent covers the use of LEM nucleic acids and polypeptides to activate T cell immunity to cancer and viral infection and agents that down-regulate LEM for the treatment of autoimmune and inflammatory disease. Retro mutant mice are available from P.G.A-R under a material transfer agreement with Imperial College London. We thank J. Hehl and S. Stoma from the Scientific Center for Optical and Electron Microscopy ScopeM of the Swiss Federal Institute of Technology ETHZ for technical support. The research was supported by the ETH Zurich, the Swiss National Science Foundation (310030_146140), MRC grant G0700795, and NIH grant AI091930. I.O. and research were supported by a grant from the Wellcome Trust; L.W. and D.H. and research were supported by a grant from Cancer Research UK (A9995); O.C. and research was supported by NIH grant AI45108. R.H. was supported by a MRC PhD studentship, and C.M. was supported by a British Heart Foundation Fellowship (FS/12/38/29640).

## SUPPLEMENTARY MATERIALS

www.sciencemag.org/cgi/content/full/science.aaa7516/DC1
Materials and Methods
Figs. S1 to 19
Tables S1 to S3
References (*31*–*38*)

23 January 2015; accepted 6 April 2015
Published online 16 April 2015
10.1126/science.aaa7516

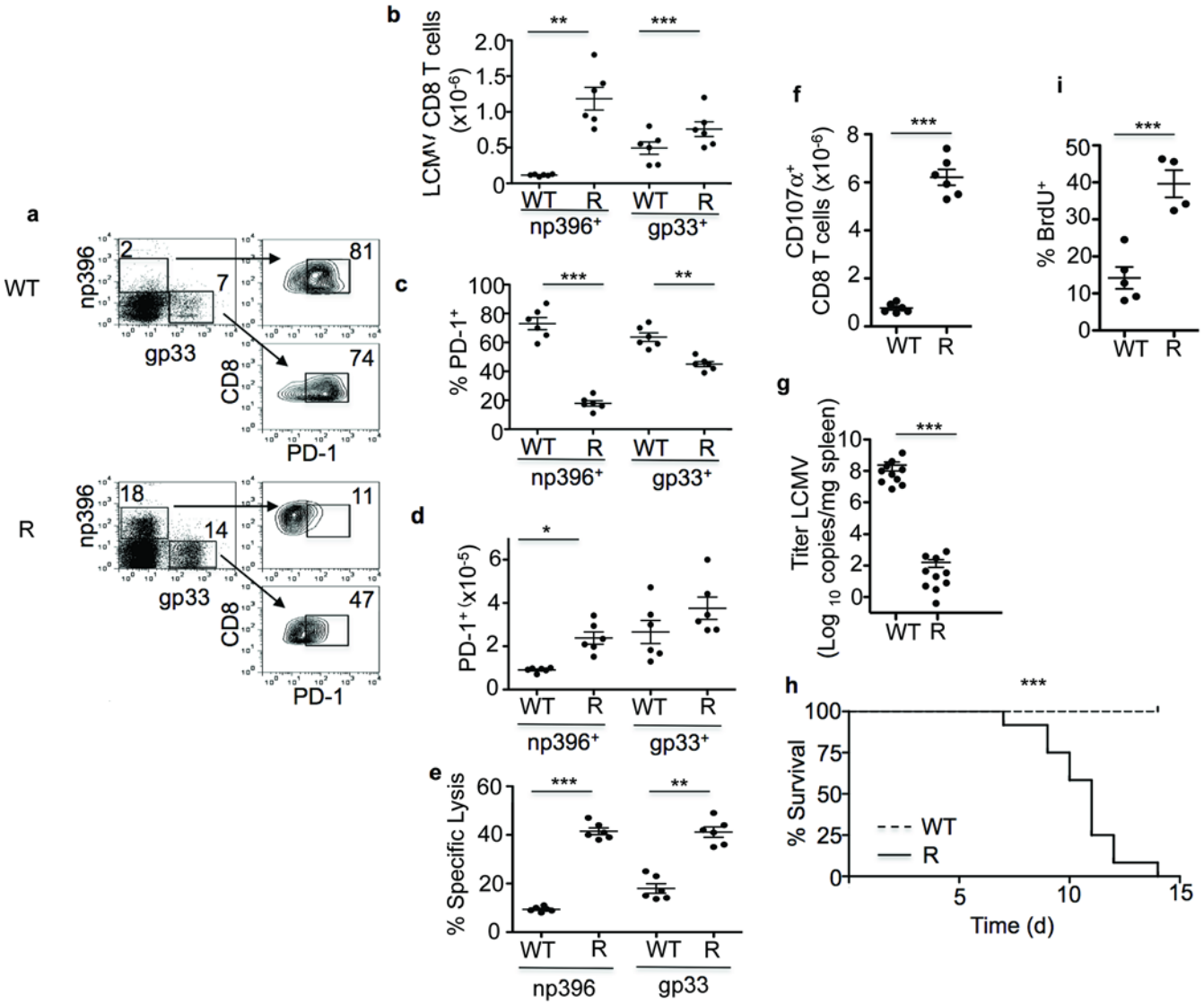


**Fig. 1. *Retro* mutant mice exhibit enhanced CD8 T cell responses to chronic LCMV infection.** (**A**) Flow cytometry on spleen cells from day 8 post infection (p.i.) with LCMV C13 of wild-type (WT) and *Retro* homozygous mutant (R) mice. Staining with tetramers, refolded with either np396 or gp33 peptides, and PD-1 is shown (% next to gate) on $CD8^+$ gated cells. (**B**) Number of $tetramer^+$ $CD8^+$ splenocytes on day 8 p.i. (**C**) % $PD\text{-}1^+$ of $tetramer^+$ $CD8^+$ splenocytes on day 8 p.i. (**D**) Number of $PD\text{-}1^+$ $tetramer^+$ $CD8^+$ splenocytes on day 8 p.i. (**E**) % specific CTL lysis from $Cr^{51}$-release assays for splenocytes on day 8 p.i. (**F**) Number of $CD107\alpha^+$ $CD8^+$ splenocytes on day 8 p.i. (**G**) Titer of LCMV C13 in the spleen on day 8 p.i. (**H**) Kaplan-Meier survival graph after LCMV C13 infection. (**I**) % $BrdU^+$ of $np396^+$ $CD8^+$ splenocytes on day 8 p.i. Mean ± sem *N* = 6-12 mice. ***$P < 0.0001$, **$P < 0.0005$, *$P < 0.001$. Two-tailed student *t* tests were used for all expect Geha-Breslow-Wilcoxon that were used for survival curves. Each data set is representative of at least 3 individual experiments.

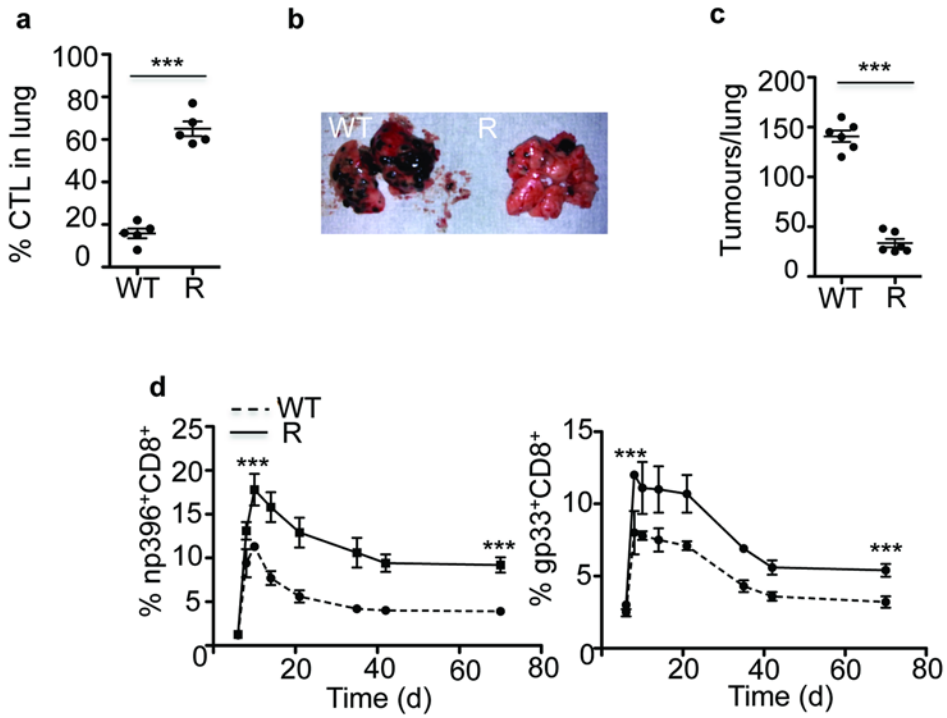


**Fig. 2. *Retro* improves immunity against tumors and acute viral infections.** Mice were injected i.v. with B16 F10 melanoma cells. (**A**) % $CD3^+$ $CD8^+$ $CD44^{hi}$ cells from lungs day 35 p.i. (**B**) Foci of melanomas in the lung on day 35 p.i. (**C**) Number of melanomas per lung on day 35 p.i. Mice were infected with LCMV Armstrong. Mean % of (**D**) $np396^+$ and (**E**) $gp33^+$ $CD8^+$ peripheral blood leukocytes (PBL). Mean ± sem, $N$ = 6-10 mice. ***$P < 0.0001$ Two-tailed student $t$ tests were used for all. Each data set is representative of at least 3 individual experiments.

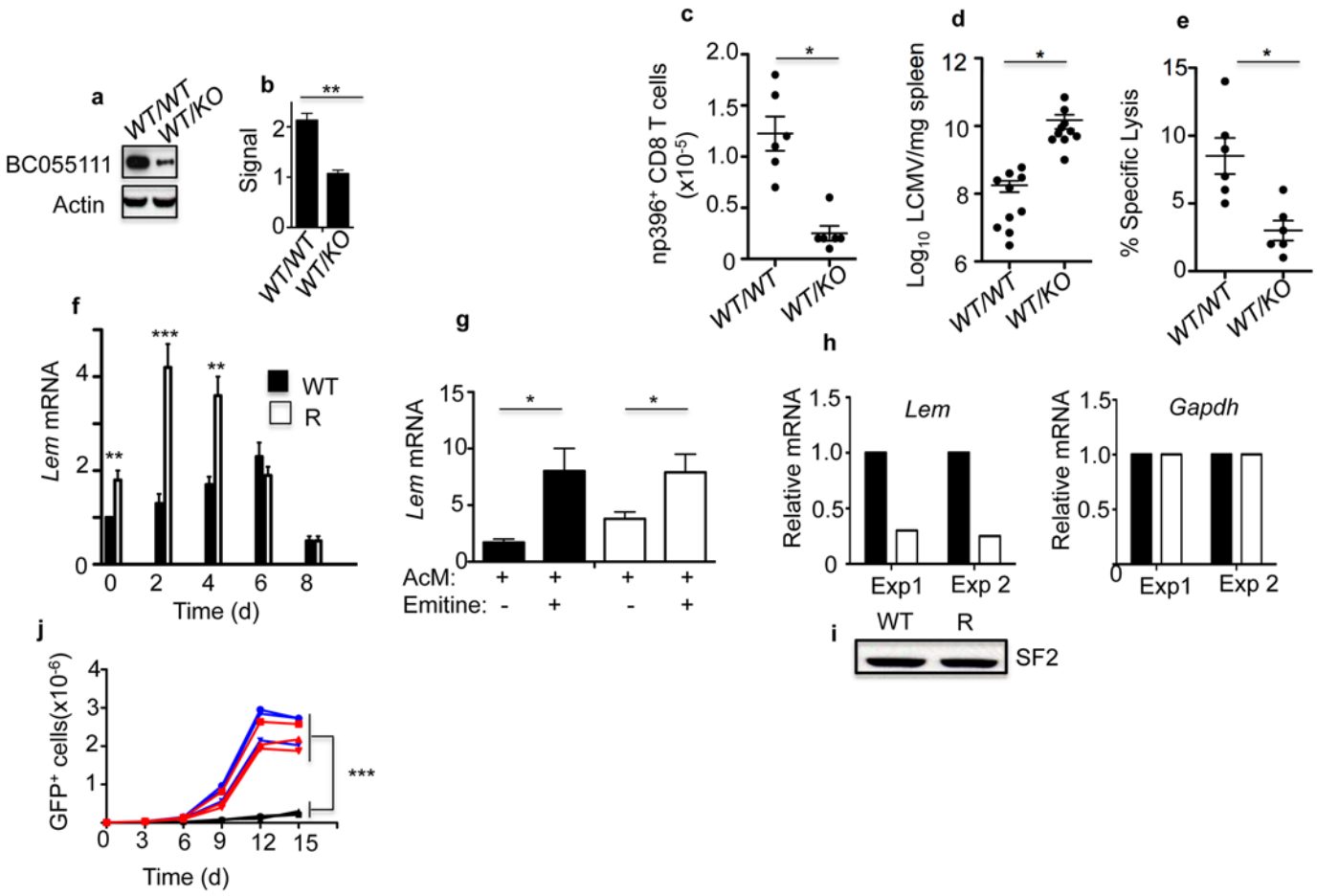


Fig. 3. ***Retro*** **mutation identifies LEM.** *BC055111*$^{W/W}$ and *BC055111*$^{W/KO}$ mice were infected with LCMV C13. (**A**) Western blot on CTL for BC055111 (49 kD) on total CD8 T cells from the spleen on day 4 p.i. (**B**) Bar graph of BC055111 signal strength from a. *BC055111*$^{W/W}$ and *BC055111*$^{W/KO}$ mice were infected with LCMV C13. (**C**) Number of np396$^{+}$ CD8$^{+}$ splenocytes on day 8 p.i. (**D**) LCMV titer in the spleen on day 8 p.i. (**E**) % specific CTL lysis from $Cr^{51}$-release assays for splenocytes on day 8 p.i. (**F**) Bar graph for mean *Lem* mRNA in total CD8 T cells from the spleens of WT or R mice after infection with LCMV C13. Level of mRNA normalized to the $t$ = 0 WT level. (**G**) Bar graphs for mean *Lem* mRNA in CD8 T cells cultured for 3 days in cytokines then incubated with actinomycin D or emitine. Level of mRNA normalized to the $t$ = 0 WT level. [(A) to (G)] Mean ± sem, $N$ = 6 mice. Each data set is representative of at least 3 individual experiments. (**H**) Bar graphs for mean relative *Lem* or *Gapdh* mRNA from 2 independent immunoprecipitation experiments performed on $N$ = 2 mice each time. mRNA levels are relative to WT and are from CD8 T cells cultured for 3 days in cytokines. (**I**) Western blot for SF2 (27 kD) after immunoprecipitation in (H). (**J**) Mean number of GFP$^{+}$ CTLL-2 cells cultured in IL-2 ($N$ = 4 wells) from 3 independent transductions with MIGR1 alone (V-black), or MIGR1 encoded *Lem* ORF (WT-blue or R- red sequence). ***$P$ < 0.005, **$P$ < 0.01, *$P$ < 0.05. Two-tailed student $t$ tests were used.

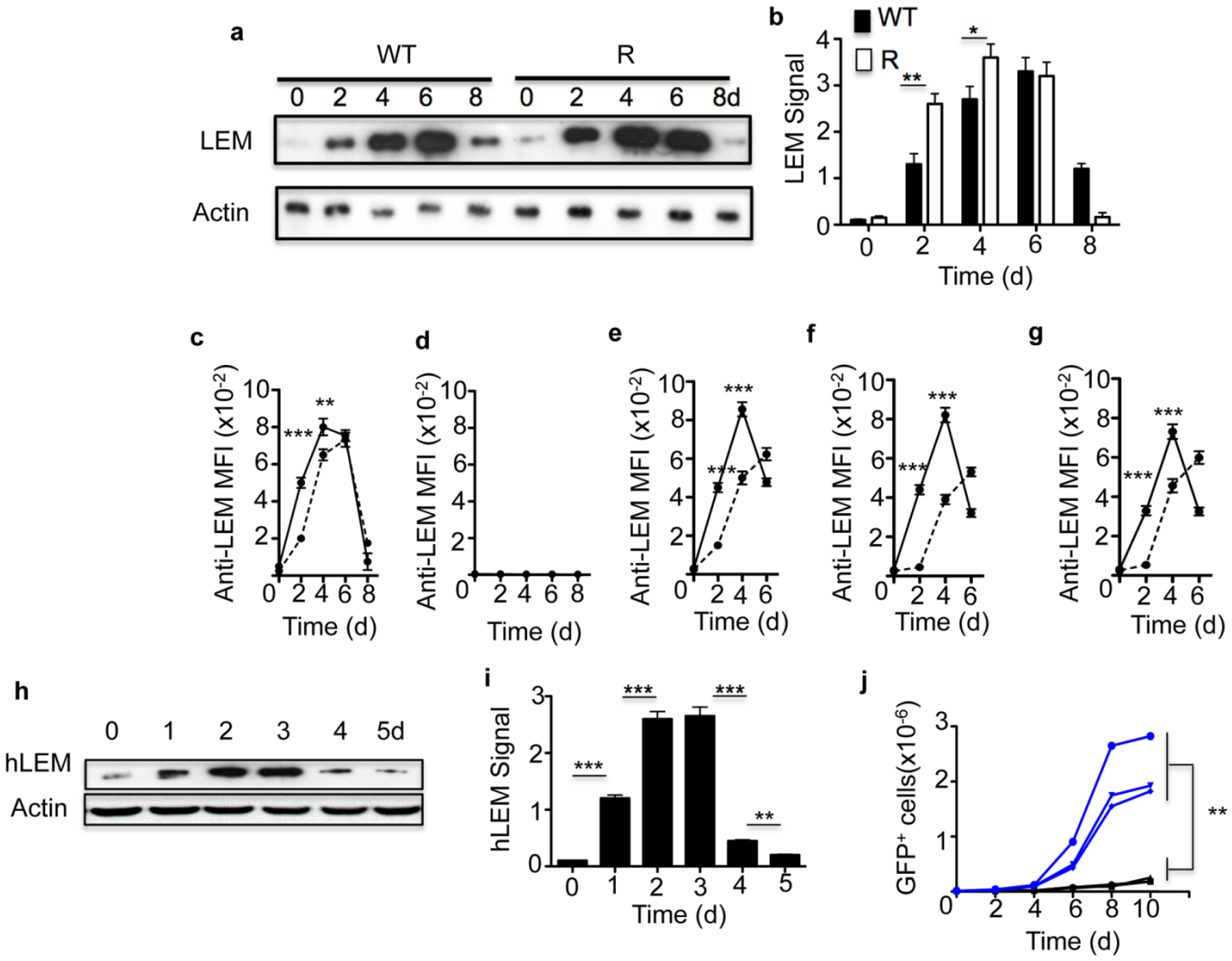


**Fig. 4. The *Retro* mutation increases LEM expression.** Mice were infected with LCMV C13. (**A**) Western blots for LEM (49 kD) on total CD8 T cells from the spleen. (**B**) Bar graph of signal strength from (A). (**C** to **G**) Mean Fluorescence Intensity (MFI) after staining with anti-LEM antibody in gated (C) $CD44^{hi}$ $CD62L^{lo}$ $CD8^{+}$ or (D) $CD44^{lo}$ $CD62L^{hi}$ $CD8^{+}$ splenocytes after infection with LCMV C13, or on total CD8 T cells that were activated in vitro with either (E) anti-CD3/CD28, (F) IL-2, or (G) IL-15. [(A) to (G)] Mean ± sem, $N = 6$ mice. (**H**) Western blots for hLEM, 49 kD on anti-CD3/CD28 activated human CD8 T cells. (**I**) Bar graph of signal strength from (H). (**J**) Mean number of $GFP^{+}$ human CD8 T cell blasts ($N = 4$ wells) after 3 independent transductions with MIGR1 alone (V-black), or MIGR1 encoded *hLEM* ORF (blue). $^{***}P < 0.0001$, $^{**}P < 0.0005$, $^{*}P < 0.001$. Two-tailed student *t* tests were used. Each data set is representative of at least 3 individual experiments.

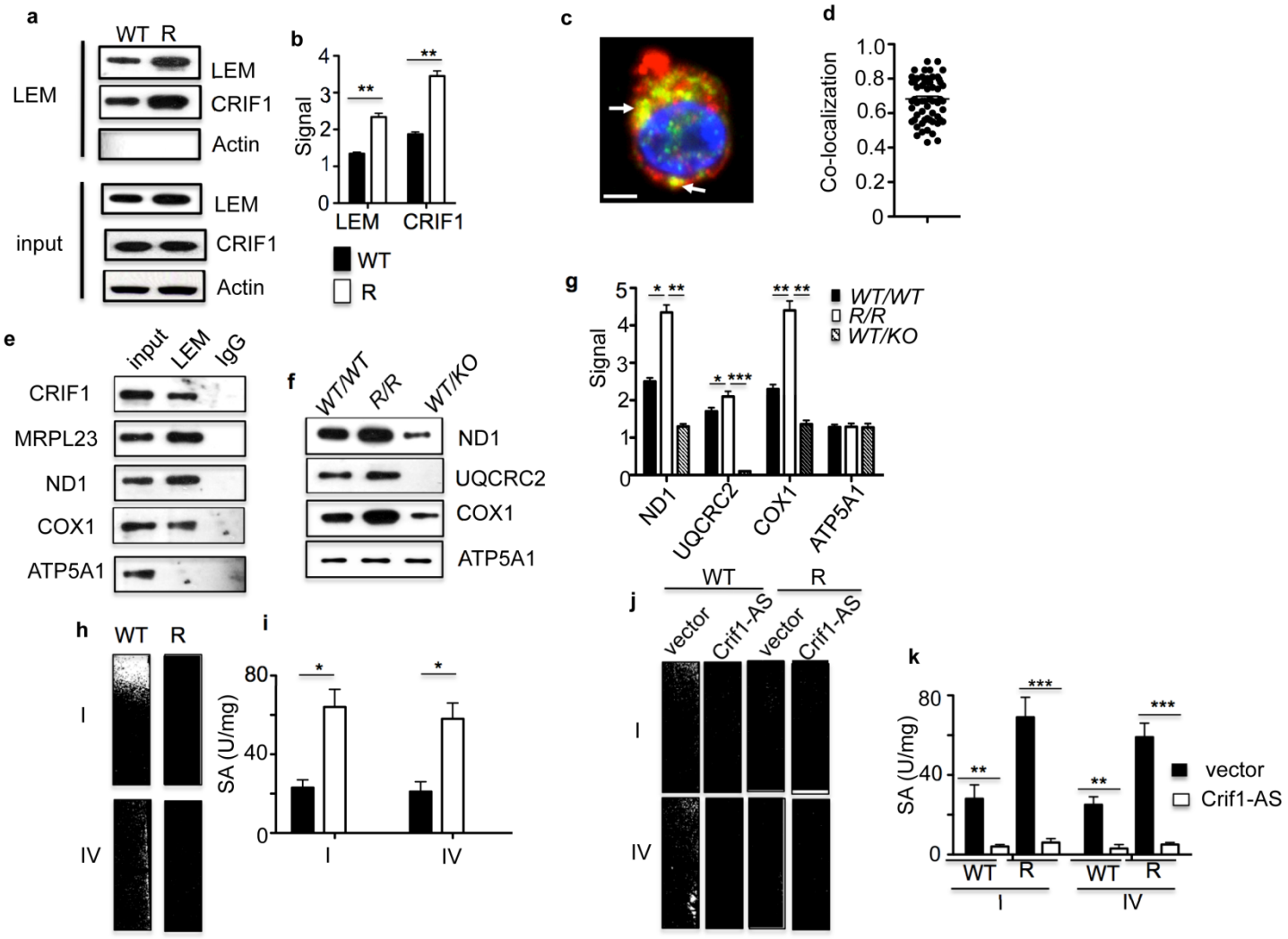


**Fig. 5. LEM interacts with CRIF1 to control the activity of OXPHOS proteins.** WT and R mice were infected with LCMV C13 and on day 4 p.i. total CD8 T cells purified. (**A**) Western blots directly on cell extracts (input) or after immunoprecipitation for LEM (LEM: 49 kD; CRIF1 25 kD; β actin 42 kD). (**B**) Bar graph of signal strengths from (A). (**C**) CIM from staining with antibodies against LEM (red) or CRIF1 (green). Nuclei stained with DAPI (blue). Examples of co-localization (yellow) are indicated by arrows. Bar = 2.5 μm. (**D**) Co-localization of LEM and CRIF1 as measured by Pearson's correlation coefficient in multiple optical cell slices ($N$ = 62). Mean = 0.68 ± 0.11. WT mice were infected with LCMV C13 and on day 4 p.i. total CD8 T cells purified. (**E**) Western blots directly on cell extracts (input) or after immunoprecipitation with LEM antibody or with control rabbit IgG (MRPL23-18 kD, ND1 36 kD, COX1 57 kD, ATP5A1 60 kD). $Lem^{WT/WT}$, $Lem^{R/R}$, or $Lem^{WT/KO}$ mice were infected with LCMV C13 and on day 4 p.i. total CD8 T cells purified. (**F**) Western blots for OXPHOS proteins (UQCRC2 49 kD.) (**G**) Bar graph of signal strength from f. WT and R mice were infected with LCMV C13 and on day 4 p.i. total CD8 T cells purified. (**H**) Immunocapture-enzyme assays for OXPHOS complexes I and IV. (**I**) Bar graphs for mean specific activity (signal strength /mg protein) from (H). Donor CD8 T cells harboring vector alone of Crif1-AS were purified from WT recipient mice on day 4 p.i. with LCMV C13. (**J**) Immunocapture-enzyme assays for OXPHOS complexes I and IV. (**K**) Bar graphs for mean specific activity from (J); mean ± sem; $N$ = 6 mice. ***$P$ < 0.005, **$P$ < 0.01, *$P$ < 0.05. Two-tailed student $t$ tests were used. Each data set is representative of at least 3 individual experiments.

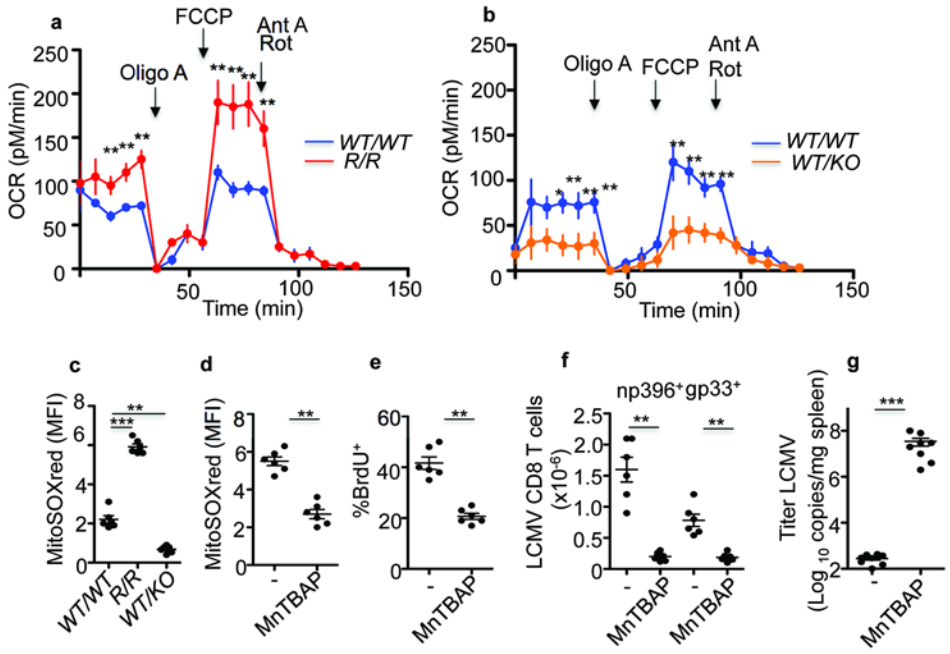


**Fig. 6. LEM controls production of mitogenic mROS.** *Lem*$^{WT/WT}$, *Lem*$^{R/R}$ or *Lem*$^{WT/KO}$ mice were infected with LCMV C13 and on day 4 p.i. total CD8 T cells purified from the spleen. (**A** and **B**) Oxygen consumption rate (OCR) after sequential injection of oligomycin, FCCP, and antimycin A/rotenone. (**C**) *Lem*$^{WT/WT}$, *Lem*$^{R/R}$ or *Lem*$^{WT/KO}$ mice were infected with LCMV C13 then on day 8 p.i. np 396$^{+}$ CD8$^{+}$ splenocytes were gated then the MFI of MitoSOX red staining determined. R mice were infected with LCMV C13 then over the course of 8 days injected with MnTBAP or not. Gated np 396$^{+}$ CD8$^{+}$ splenocytes were examined on day 8 p.i. for (**D**) MitoSOX red staining and (**E**) % BrdU-positive cells. In the same spleens, (**F**) Number of tetramer-positive cells. (**G**) Titer of LCMV. Mean ± sem. For (A) to (F), $N = 6$ mice and g $N = 9$ mice. ***$P < 0.001$, **$P < 0.005$, *$P < 0.01$. Two-tailed student $t$ tests were used. Each data set is representative of at least 3 individual experiments.